EFDA–JET–CP(09)06/20

P. Buratti, R.J. Buttery, C.D. Challis, I.T. Chapman, F. Crisanti, M. Gryaznevich,
T.C. Hender, D.F. Howell, E. Joffrin, J. Hobirk, F. Imbeaux, X. Litaudon,
J. Mailloux and JET EFDA contributors

MHD Stability Limit Analysis in JET High β_N Advanced Scenarios

MHD Stability Limit Analysis in JET High β_N Advanced Scenarios

P. Buratti[1], R.J. Buttery[2], C.D. Challis[2], I.T. Chapman[2], F. Crisanti[1], M. Gryaznevich[2], T.C. Hender[2], D.F. Howell[2], E. Joffrin[3], J. Hobirk[4], F. Imbeaux[3], X. Litaudon[3], J. Mailloux[2] and JET EFDA contributors*

JET-EFDA, Culham Science Centre, OX14 3DB, Abingdon, UK

[1]EURATOM-ENEA Fusion Association, C.R. Frascati, CP65, 00044 Frascati, Italy
[2]EURATOM-UKAEA Fusion Association, Culham Science Centre, OX14 3DB, Abingdon, OXON, UK
[3]Association EURATOM-CEA, 13108 St Paul-lez-Durance, France
[4]EURATOM Assoziation Max-Planck-Institut für Plasmaphysik, Boltzmannstrasse 2, 85748 Garching, Germany,
** See annex of F. Romanelli et al, "Overview of JET Results",*
(Proc. 22 [nd] IAEA Fusion Energy Conference, Geneva, Switzerland (2008)).

Preprint of Paper to be submitted for publication in Proceedings of the
36th EPS Conference on Plasma Physics, Sofia, Bulgaria.
(29th June 2009 - 3rd July 2009)

1. INTRODUCTION

High β_N plasmas with q and pressure profiles ranging from Hybrid to ITB shapes (min q from 1 to above 2) have been explored in JET experiments on advanced regimes. Various instabilities were observed, including ideal-like modes with toroidal Number n = 1 [1] and Tearing Modes (NTMs) with m/n = 2/1, 3/2, 4/3, up to n = 6. In the hybrid regime in particular, modes with 3 < n had detrimental effects on confinement, and a large part of the experimental effort was spent to reach relatively stable conditions with only n ≥ 3 modes [2]. Furthermore, the n = 1 mode was the main obstacle to the prolongation of high β_N phases, when this parameter was pushed towards the maximum value in each regime [3, 4]. The n = 1 mode at high β_N featured some characteristics in common with the Resistive Wall Mode (RWM), i.e. initial slow growth in the absence of magnetic reconnection, and some others in common with energetic particle modes, like the possible occurrence in the form of fishbone-like bursts.

2. CHARACTERISTICS OF THE N = 1 MODE

Spectrograms of magnetic coils signals revealed three different kinds of n = 1 modes, namely continuous oscillations at frequencies corresponding to bulk plasma rotation, fishbone-like bursts and broadband activity. The continuous oscillation has m = 2 dominant poloidal number and grows at first without reconnection (see next section). Bursts have similar structure, which leads to identify them as q = 2 fishbones. Similar results from DIII-D and JT-60U were reported in [5, 6]. The broadband activity occurs around the top frequency of fishbone bursts. Fig.1 shows that fishbones occur at min q around 2 and the highest β_N values are reached at 1 $q_{\min}$. In this range stable and unstable points are mixed; furthermore, the instability appears in many cases while β_N is constant, showing that β_N is not an absolute stability parameter. Fig.2 shows that some separation between stable and unstable points is given by the ion diamagnetic frequency

$$\omega_{*pi} = -\,(n/eN)\; dP_i/d\psi \approx -\,(m/rB)\; dT_{i[eV]}/dR$$

with more unstable points at higher ω_{*pi}.

3. RADIAL STRUCTURE OF THE N = 1 MODE

The radial structure of temperature perturbations has been analysed using 48 fast channels from the Electron Cyclotron Emission (ECE) diagnostic. Phase profiles were extracted from cross-spectral density with a reference magnetic signal [1]. The slope of phase profiles gives information on the poloidal harmonic composition of the mode. The dominant harmonic was m = 2, while a secondary m = 1 component was detected in the central region at $q_{min} \approx 1$. Most important, magnetic islands can be detected from π-jumps between nearby channels. Modes considered in this paper grow to a significant fraction of the saturation amplitude without developing any magnetic island; this is the main characteristic that distinguishes these instabilities from the 2/1 NTM [7]. Figure 3 displays phase evolution in radius and time. No island is detected during the first 0.2s of mode growth, i.e. at this stage the mode has kink-like structure. A π-jump (red-blue transition in the color map) develops between 0.2 and 0.4s. During this mixed kink-tearing stage the phase of ECE channels

that detect the island changes progressively (see green trace in Fig.3d) implying that the tearing component has a phase lag with respect to the kink one [1]. One possible explanation of this phase lag is that the island is formed in consequence of forced reconnection [8] driven by the kink displacement.

4. AMPLITUDE EVOLUTION AND BALLOONING STRUCTURE

During the non-reconnecting stage the mode structure is similar to that of kink modes that disrupt discharges with very peaked pressure profile ($P_0/\langle P\rangle \approx 7$) but, in these H-mode plasmas with moderate pressure peaking $P_0/\langle P\rangle < 4$), the mode growth is slow. The blue trace in Fig.4 shows mode amplitude from a magnetic coil on the Low Field Side (LFS). Signal growth is compatible with an exponential with $\gamma = 10s^{-1}$; saturation occurs in 0.2s. Spikes before $t = 6.3$s are $q = 2$ fishbones (in this case the continuous mode starts just after a fishbone, but in many other cases there is no coincidence with any possible trigger event). The red trace in Fig.4 shows signal from a coil on the High Field Side (HFS) having nearly the same radial distance from the magnetic axis as the other coil. At first the mode has ballooning character, in fact the HFS signal is much smaller than the LFS one. After island formation (vertical dashed line), the ballooning asymmetry gradually disappears.

SUMMARY AND DISCUSSION

The experimental findings can be summarized as follows

1) The n=1 mode features a non-reconnecting stage
2) The mode has strong ballooning character during this stage
3) The growth rate is quite small
4) The mode frequency is much larger than the inverse wall time, $\omega\tau_{wall} \approx 10^2$
5) Plasmas with larger ω_{*pi} tend to be more unstable

The initial absence of reconnection implies that the mode can not tap energy from the magnetic field. The remaining possible energy sources are thermal pressure gradient and fastparticles pressure gradient. The latter could play a relevant role as in these experiments the suprathermal pressure fraction typically was of 30%. Furthermore, the existence of $q = 2$ fishbones indicates that, at least in some conditions (i.e. $q_{\min} \approx 2$), fast particles can drive the mode. The dispersion relation relevant for both fishbones and RWM is of the form [9, 10]

$$-iK(\omega) + \delta W_k(\ ) + \delta W_b = O(1/\ \tau_{wall}), \qquad (1)$$

where δW_b (δW_k) are fluid (kinetic) energy perturbations and K represents plasma inertia. The r.h.s. is dominant for the quasi-static RWM, but in this case its contribution is non negligible only if the l.h.s. gives neutral stability. In the relevant frequency range, $\delta W_w(\omega)$ has negative contributions both from thermal ions [11] and from precession resonance of fast trapped ions; the necessary condition for instability Re $\delta W_w(\omega) + \delta W_b < 0$ can then be satisfied if δW_b is not too large [9]. A progressive decrease of δW_b (due to profiles evolution) could explain the instability onset at constant beta.

The role of fast particles is less clear for the continuous mode. The concentration of unstable cases at higher ω_{*pi} (Fig.2) could be due to the fact that the shear-Alfvén continuum accumulation

point K ($\omega \approx \omega_{*pi}$) = 0 [9] meets stronger fast-ions resonance effects. In alternative, since higher ω_{*pi} is associated with stronger pressure gradient, ideal instabilities of the infernal type could be excited. Further analysis is needed to resolve this point.

In conclusion, the observed n = 1 mode can be more unstable than the RWM, as it does not require global no-wall ideal instability, nor it is damped by plasma rotation.

ACKNOWLEDGEMENTS

This work, supported by the European Communities under the EURATOM/ENEA contract of Association, was carried out within the framework of the European Fusion Development Agreement. The views and opinions expressed herein do not necessarily reflect those of the European Commission.

REFERENCES

[1]. P. Buratti et al., 35th EPS Conf. on Plasma Physics ECA 32D (2008) P1.069

[2]. J. Hobirk et al., this Conference O5.057

[3]. C.D. Challis et al., this Conference P5.172 [4] J. Mailloux et al., this Conference, P5.164

[5]. M. Okabayashi et al., 22nd IAEA Fusion Energy Conference (2008) EX/P9-5

[6]. G. Matsunaga et al., 22nd IAEA Fusion Energy Conference (2008) EX/5-2

[7]. P. Maget, this Conference P**5**.179

[8]. R. Fitzpatrick, T.C.Hender, Phys. Fluids B **3**, 644 (1991)

[9]. F. Zonca et al., Phys. Plasmas **6**, 1917 (1999)

[10]. Y. Liu et al., Phys. Plasmas **16**, 056113 (2009)

[11]. Y. Liu et al., Phys. Plasmas **15**, 092505 (2008)

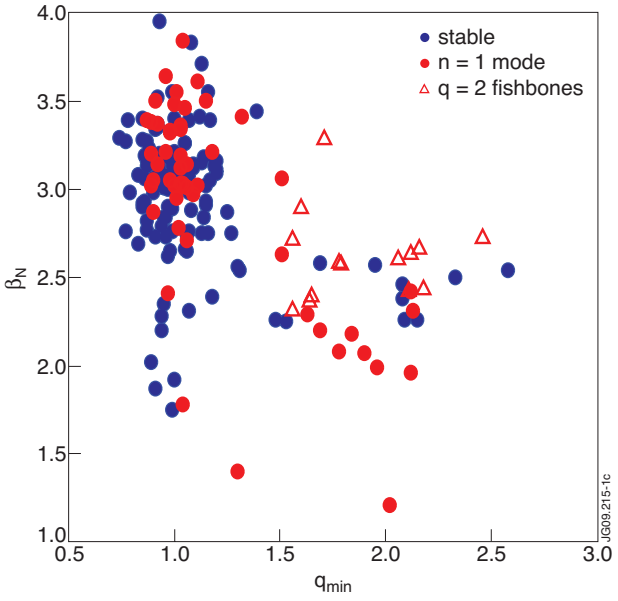

Figure 1: β_N at instability onset (maximum attained value for stable discharges) versus minimum q from MSE diagnostic.

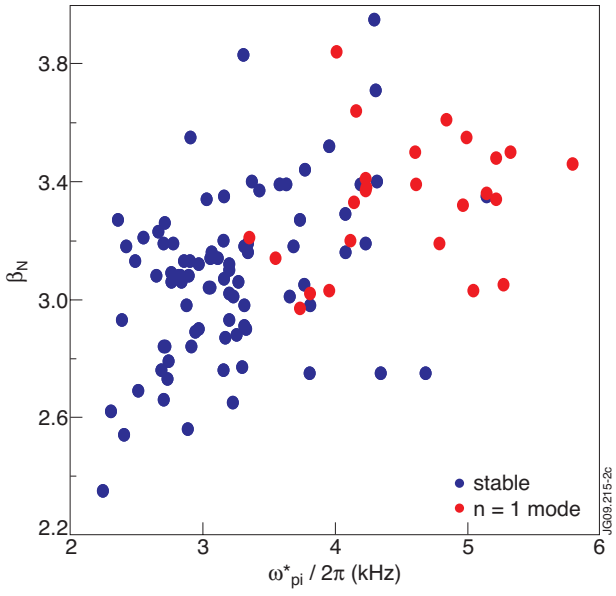

Figure 2: β_N at instability onset (maximum attained value for stable discharges) versus ω_* at mid radius. Data are selected with triangularity δ>0.25, q_{min}<1.5 and presence of ELMs.

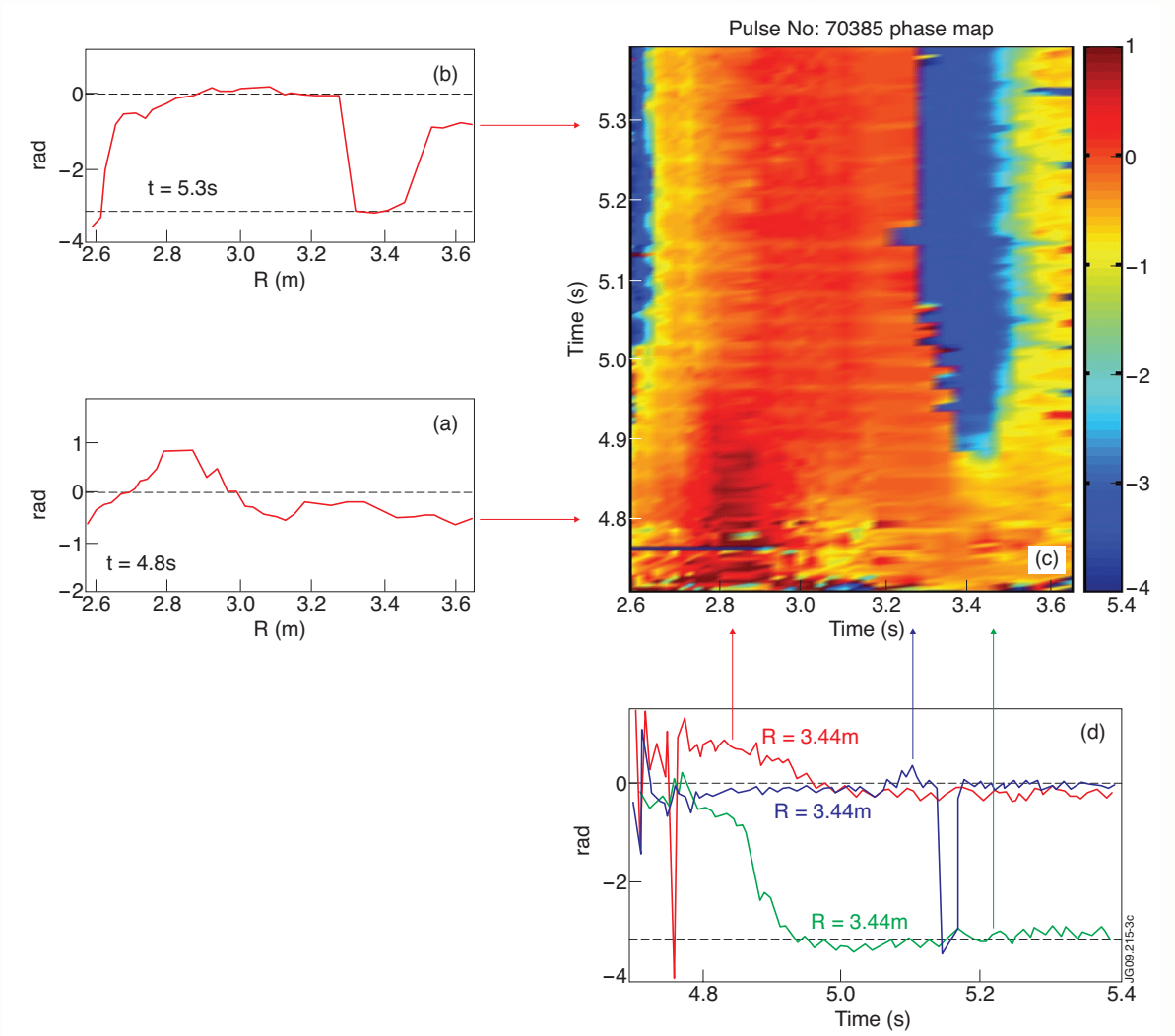

Figure 3: Phase evolution and profiles at the n = 1 mode frequency (9kHz) with m = 2 baseline subtracted. a) Profile during the nonreconnecting stage. b) Profile after full reconnection. c) Full radius-time map. d) Phase evolution at three radii. Arrows point to times of profiles and radii of time traces in the full map.

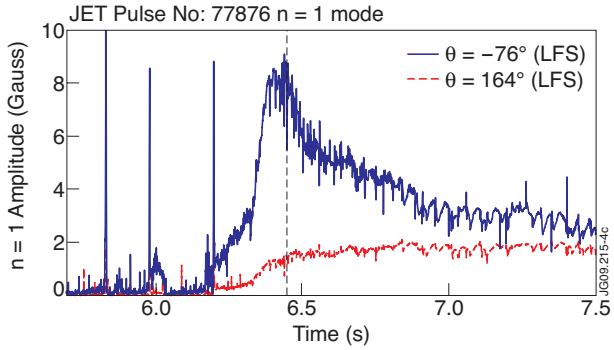

Figure 4. Low and high field side magnetic field perturbation. The dashed line marks island formation time. θ is coil poloidal location with respect to the magnetic axis.